HHS Public Access

Author manuscript

J Neurosci Res. Author manuscript; available in PMC 2018 April 01.

Published in final edited form as:

J Neurosci Res. 2017 October ; 95(10): 1937–1950. doi:10.1002/jnr.24056.

Otoprotective Effects of Mouse Nerve Growth Factor in DBA/2J Mice with Early-Onset Progressive Hearing Loss

Qingzhu Wang[a,b,1], **Hongchun Zhao**[b,1], **Tihua Zheng**[a,1], **Wenjun Wang**[a,b,c,1], **Xiaolin Zhang**[b], **Andi Wang**[c], **Bo Li**[a], **Yanfei Wang**[a,b,**], and **Qingyin Zheng**[c,*]

[a]Transformative Otology and Neuroscience Center, Binzhou Medical University, Yantai 264003, Shandong, PR China

[b]Department of Otolaryngology/Head and Neck Surgery, Institute of Otolaryngology, Affiliated Hospital of Binzhou Medical University, Binzhou 256600, Shandong, PR China

[c]Department of Otolaryngology-HNS, Case Western Reserve University, Cleveland, OH 44106, USA

Abstract

DBA/2J is an inbred mouse strain widely used in hearing research, as it displays progressive hair cell loss and degeneration of spiral ganglion neurons (SGNs) characterized by early-onset progressive hearing loss (ePHL). Mouse nerve growth factor (mNGF), as a common exogenous nerve growth factor (NGF), has been studied extensively for its ability to promote neuronal survival and growth. To determine whether mNGF can ameliorate progressive hearing loss (PHL) in DBA/2J mice, saline or mNGF was given to DBA/2J mice of either sex by daily intramuscular injection from the 1st to the 9th week after birth. At 5, 7, and 9 weeks of age, in comparison with vehicle groups, mNGF groups experienced decreased auditory-evoked brainstem response (ABR) thresholds and increased distortion product otoacoustic emission (DPOAE) amplitudes, the prevention of hair cell loss, and the inhibition of apoptosis of SGNs. Downregulation of *Bak*/*Bax* and *Caspase* genes and proteins in cochleae of mice receiving the mNGF treatment was detected by Real-time PCR, Western Blot and Immunohistochemistry. This suggests that the Bak-dependent mitochondrial apoptosis pathway may be involved in the otoprotective mechanism of mNGF in progressive hearing loss of DBA/2J mice. Our results demonstrate that mNGF can act as an otoprotectant in the DBA/2J mice for the early intervention of PHL and, thus, could become of great value in clinical applications.

Graphical abstract

[*]Corresponding author. Department of Otolaryngology-HNS, Case Western Reserve University, 11100 Euclid Avenue, LKS 5045, Cleveland, OH 44106, USA. qyz@case.edu (Q. Zheng). [**]Corresponding author. Department of Otolaryngology/Head and Neck Surgery, Institute of Otolaryngology, Affiliated Hospital of Binzhou Medical University, Binzhou 256600, Shandong, PR China. entwyf@163.com (Y. Wang).

[1]These authors contributed equally to this work.

Conflict of Interest Statement

The authors declare that no conflict of interest exists.

Author's roles

Qingzhu Wang, Yanfei Wang, and Qingyin Zheng conceived and designed the experiments; Qingzhu Wang, Tihua Zheng, Xiaolin Zhang, Hongchun Zhao, Andi Wang, Tianhe Xu and Bo Li performed the experiments and analyzed the data; and Qingzhu Wang, Wenjun Wang and Qingyin Zheng wrote the paper.

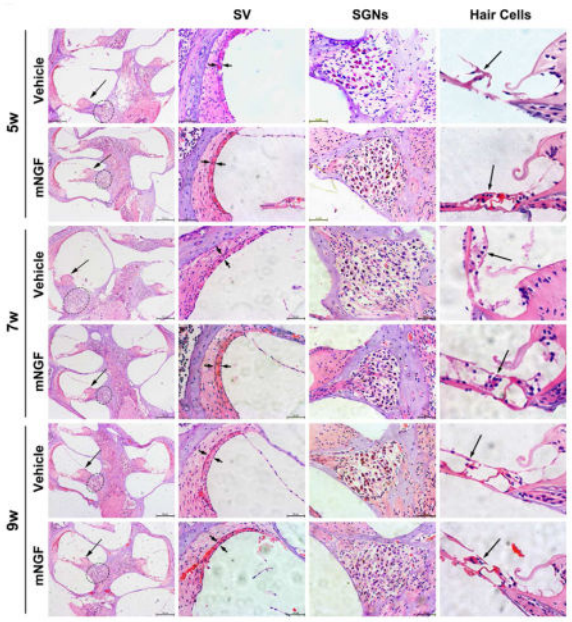

mNGF can inhibit apoptosis of the spiral ganglion cells, prevent degeneration of stria vascularis and protect the hair cells. Ultimately, mNGF protect the age related hearing loss in the DBA/2J mice.

Keywords

mouse nerve growth factor; progressive hearing loss; mouse model; hair cells; spiral ganglion neurons; apoptosis; mitochondrial pathway

Introduction

Over 5% of the world's population – 360 million people – suffers from disabling hearing loss (WHO Fact sheet). Currently, there is no effective FDA-approved drug to treat hearing loss. Mouse models play a crucial role in understanding the pathogenesis associated with hearing disorders (Angeli et al. 2012), among which the DBA/2J mouse strain is one of the most widely used models for hearing research (Johnson et al. 2008). The DBA/2J mouse strain harbors the *Cdh23*^{753A} (*ahl*) variant and a missense mutation of the *fascin-2* gene (*ahl8*, or *Fscn2*^{R109H}), both of which affect hair cell stereociliary bundle function and stability (Johnson et al. 2008; Shin et al. 2010). CDH23 is a component of stereocilia tip link and the FSCN2 protein is an abundant actin crosslinker in hair-cell stereocilia. *Fscn2*^{R109H} is unique to the DBA/2J inbred strain and accelerates hearing loss only in the presence of *Cdh23*^{ahl} homozygous, which causes a much earlier onset and more rapid progression of hearing loss than C57BL/6J mice (that only have the *Cdh23*^{ahl} allele). A QTL on Chr 5 (*M5ahl8*) modifies its effect on the severity of hearing loss associated with the *Fscn2*^{R109H} variant. (Johnson et al. 2015) The hearing loss in the DBA/2J mice strain begins at approximately 3 weeks of age, with deterioration to total deafness by 3 months of age, as we previously reported (Johnson et al. 2008; Zheng et al. 1999). In DBA/2J mice, hearing loss

begins in the high-frequency region and progressively spreads toward the low frequencies, accompanied by progressive degeneration of hair cells and spiral ganglion neurons (SGNs) that begin at the base turn and spread to the apex of the cochlea (Someya et al. 2009). A recent study showed that the apoptosis of neurons caused by mitochondrial dysfunction contributes to hearing loss (Raimundo et al. 2012).

Nerve growth factor (NGF) is one of the most well-studied neurotrophic factors to date. A study showed that NGF is essential for viability, differentiation, and maintenance in nerve cells (Doerks et al. 2002). Additionally, it contributes to the repair of the nervous system (Verge et al. 1996). Moreover, NGF may be implicated in interactions between auditory receptors and efferent innervation of the developing cochlea (Despres et al. 1991). Tropomyosin receptor kinase (Trk) receptors are a family of tyrosine kinases that regulate synaptic strength and plasticity in the mammalian nervous system (Huang and Reichardt 2003). Trk receptors affect neuronal survival and differentiation through several signal cascades. It is suggested that NGF binds to TrkA and $p75^{NTR}$ (Bothwell 1995). Many reports have shown signals related to NGF when binding with the TrkA receptor, becoming phosphorylated and sending a signal downstream, thus causing Akt transformation to phospho-Akt, resulting in increased cell survival (Datta et al. 1997; del Peso et al. 1997; Greene and Kaplan 1995). $p75^{NTR}$ can increase the binding affinity of NGF to TrkA, thus raising the intracellular signal transduction (Hantzopoulos et al. 1994). However, the JNK/P53/Bax pro-apoptotic pathways, mediated by $p75^{NTR}$, induce the mitochondrial apoptosis and causes cell apoptosis. A study showed that overexpression of NGF and TrkA can inhibit the apoptosis function of $p75^{NTR}$ and activate the signal that promotes peripheral nerve cell survival (Park et al. 2007). During the development of the embryo, both NGF and its receptors are widely expressed in the inner ears; levels decrease after birth, and remain at low in adulthood. NGF may be involved in the differentiation of acoustic ganglion cells and hair cells (Bernd and Represa 1989). Therefore, we hypothesized that supplementation with NGF can inhibit neuron damage and can even protect against hearing loss.

To date, the only effective therapies available to treat hearing loss are hearing aids and the cochlear implant auditory prosthesis for severe hearing loss. mNGF treatment used as a preventative measure is a new method of ameliorating hearing loss, thus improving quality of life. However, clinicians cannot easily understand the usage of mNGF because of the unclear mechanism(s). As such, the aim of our study was to evaluate the ameliorative effects produced by mNGF on auditory dysfunction in a progressive hearing loss model and provide evidence of the possible mechanism(s) related to mNGF in auditory neural protection and survival by evaluating genes/proteins to be altered by mNGF with Real-time PCR, Western Blot and Immunohistochemistry.

Materials and Methods

Mouse Preparation

DBA/2J mice (RRID: IMSR_JAX:000671) were originally purchased from the Model Animal Research Center of Nanjing University (Nanjing, P.R. China) and then relocated to Binzhou Medical University (Yantai, Shandong, P.R. China) for breeding in specific pathogen-free animal rooms. The room temperature was maintained at 24±1°C and

sufficient food and water were provided. A total of 186 DBA/2J mice aged 1 week were divided into the mNGF-treated group (n=78), the vehicle group (n=78) and the non-treated group (n=30). The animal studies were conducted in accordance with the principles set forth in the Guide for the Care and Use of Laboratory Animals of Binzhou Medical University and were approved by the Institutional Animal Use and Care Committee of Binzhou Medical University. The classic exogenous NGF, mouse nerve growth factor (mNGF), is extracted from the submaxillary gland of male mice and shares more than a 90% homologous amino acid sequence with the NGF of humans. A saline solution of mNGF was administered by intramuscular injection (64.8 μg/kg daily) to mice that were 1 to 9 weeks old, as the manufacturer instructed (S20060052 Sinobioway Medicine, Xiamen, China).

Auditory-evoked brainstem response (ABR) and distortion product oto-acoustic emission (DPOAE)

The ABR of the DBA/2J mice was measured at 5 weeks, 7 weeks, and 9 weeks of age in the mNGF-treated group, the vehicle group and the non-treated group (male 5, female 5, n=10 for each group), by a person blind to the treatments. A computer-aided evoked potential system (Intelligent Hearing Systems, Miami, FL, USA) was used to test mice for ABR thresholds, as previously described (Zhang et al. 2015; Zheng et al. 1999). Briefly, mice were anesthetized with 4% chloral hydrate, and body temperature was maintained at 37–38°C by placing them on a heating pad in a sound-attenuating chamber. Subdermal needle electrodes were inserted at the vertex (active) and ventrolaterally to (reference) the right ear and to the left ear (ground). Clicks and 8-, 16-, and 32-kHz tone bursts were channeled through plastic tubes into the animals' ear canals. Alternating clicks (0.1ms duration) were delivered through earphones (Etymotic ER-2A) at a rate of 19.3 stimuli/s. A half cosine square window was used to create tone burst signals with a 3 ms duration (1.5 ms rise-fall with no plateau). Physiological filters were set to pass electrical activity between 100 and 3000 Hz. Monaural responses were recorded for each mouse and averaged in an 11.80 ms time window. One thousand sweeps were collected. The amplified brainstem responses were averaged by a computer and displayed on a computer screen. Auditory thresholds were obtained by decreasing the sound pressure level (SPL) by 10 dB. When finally no response was detected, the SPL was increased or decreased by 5 dB until a response was determined. Threshold was defined as the lowest intensity at which a visible ABR wave was seen. We recorded the ABR after comparing the ABR patterns with two or three suprathreshold ABRs displayed successively on the screen. ABR threshold values above 55 (for click stimulus), 40 (for 8 kHz), 35 (for 16 kHz), or 60 (for 32 kHz) dB SPL were considered hearing impaired (Han et al. 2013; Zheng et al. 1999).

To test the function of outer hair cells (OHCs) of different mice at different time points, we used the IHS Smart EP 3.30 and USB ez Software (Intelligent Hearing Systems, Miami, FL) for DPOAE measurement, which was conducted for pure tones from 4 to 36 kHz (Polak et al. 2004). Frequencies were presented with an F2/F1 ratio of 1.22. The stimuli were presented starting with the lowest frequencies tested and were increased to the highest frequencies tested. The DPOAE amplitude, which displayed as DP on the screen, was recorded after repeating two times.

After ABR and DPOAE hearing measurements were performed, all mice were used to conduct histopathological and SGNs counting (n=5), hair cell counting (n=5), TUNEL staining (n=4), real time PCR (n=5) and western blotting (n=4) or Immunohistochemistry (n=3) analyses (Fig. 1).

Histological Analyses of Inner Ears

Histological analyses of inner ears were performed following the methods described previously (Zheng et al. 2009). Briefly, the cochlea was excised, immersed in a fixative containing 4% paraformaldehyde in PBS solution for 1 day, and decalcified in 10% EDTA for 1 week. The time points selected were 5 weeks, 7 weeks, and 9 weeks of age. Sections (5 μm) were mounted on glass slides and counterstained in hematoxylin and eosin (HE). Hair cells, spiral ganglion cells, and stria vascularis were observed under light microscopy (Leica DMI4000 B, Wetzlar, Germany). SGN counts were carried out following the methods described previously (Semaan et al. 2013). The average value in four sections approaching the maximum area from a turn of each animal's cochlea was defined as the density for that turn. The SGN size was taken into account when computing the SGN packing density. The correction factor was determined by dividing the section thickness (5 μm) by the sum of the section thickness and the average diameter of the neuronal nucleus: T/T + H, where T is section thickness and H is the average nuclear diameter. The average nuclear diameter was determined separately for each group by measuring the diameter of numerous nuclei in midmodiolar sections of Rosenthal's canal selected randomly. To compare mNGF-treatment-related changes in stria vascularis width, the thickest portions of the stria vascularis were selected and measured with the aid of Image J software (http://rsb.info.nih.gov/ij/index.html, RRID:SCR_003070).

Cytocochleograms

Organs of Corti were prepared as follows: carefully micro-dissected out; subdivided into base turn, middle turn, and apex turn; and then mounted in Shandon immu-mount (Thermo) on glass slides. The surface preparations were first stained for F-actin with Alexa Fluor 488 conjugated to phalloidin (1:500 dilution) for 1 hr at room temperature, protected from light, then mounted after washing twice in 0.01M phosphate-buffered saline (1×PBS), and finally observed with a confocal fluorescence microscope (Leica DMI4000B, Leica Microsystems, Wetzlar, Germany). Hair cells were counted as present if V shapes of hair bundles were intact. The damaged/lost cells were counted in one hundred cells. Outer hair cell (OHC) were counted in the basal turns of the organs of Corti and were displayed as the percentage of missing hair cells (Han et al. 2012).

TUNEL staining

TUNEL staining for apoptotic nuclei was performed using a DeadEnd Colorimetric TUNEL System (Keygen Biotech, Jiangsu, P.R. China) according to the manufacturer's instructions. Color development was accomplished with diaminobenzidine for 4 min. Duplicate sections were counterstained with hematoxylin, and a cover glass was mounted to each slide with Permount mounting medium. For tissue sections, TUNEL-positive cells (dark brown cells) were counted in the basal regions of the cochlear sections using a ×40 objective. TUNEL-positive cells were identified by the presence of a brown-stained nucleus in the SGNs

regions. The TUNEL-positive cells were calculated as the number of TUNEL-positive cells per mm^2 with the aid of Image J software (http://rsb.info.nih.gov/ij/index.html, RRID:SCR_003070). Five sections of the unilateral basal regions were evaluated in one cochlea per mouse. Four mice were used for each mNGF-treated group and vehicle group at 5 weeks, 7 weeks, and 9 weeks of age.

Assays for Gene Transcription

Mitochondria apoptosis related genes, such as *Bak, Bax, Caspase-9*, and *Caspase-3*, were tested in this study. DBA/2J mice (n=5) at the ages of 5, 7, and 9 weeks were randomly chosen. Both bullae were removed from each mouse. Total RNA was extracted using Trizol (Roche Diagnostics, Indianapolis, IN, USA), and cDNA was made using random primers following the First-Strand Synthesis protocol (Takara Bio, Dalian, P.R. China). Real-time PCR was used to determine relative gene expression levels using FastStart Universal SYBR Green Master (Roche Diagnostics, Indianapolis, IN, USA) and the MyiQTM Real-Time PCR Detection System (Bio-Rad Laboratories, Inc., Hercules, CA, USA). The messenger RNA (mRNA) level of glyceraldehyde 3-phosphate dehydrogenase (*GAPDH*) was used as the endogenous control (Table 1).

All primers were synthesized by Sangon Biotech Co. Ltd. (Shanghai, China). Each PCR reaction contained 12.5 μl of Fast Start Universal SYBR Green Master Mix, 1 μl of cDNA, 0.75 μl of each 10 mM primer, and 7 μl of ddH_2O. The reaction conditions were as follows: denaturing at 95°C for 10 min, followed by 40 cycles of 95°C for 15 s and 60°C for 1 min. The fold change in genes relative to *GAPDH* was determined by the $2^{(-\Delta\Delta Ct)}$ method (Semaan et al. 2013).

Western Blotting

To clarify the mechanism of the effect of mNGF, we also detected the mitochondria apoptosis related proteins, such as *Bax* and *Caspase-3*. At weeks of 5, 7, and 9, mice were euthanized with chloral hydrate (1 g/kg), and both temporal bones were immediately removed. Two cochleae were homogenized in a tube containing ice-cold lysis buffer (100 mM Tris, pH 7.4, 200 mM NaCl, 1% NP-40, 10 mM $MgCl_2$) with protease inhibitors (PMSF). Lysates were incubated for 20 minutes at 37°C and then centrifuged for 30 min at 12,000 rpm at 4°C. In addition, proteins in the supernatant were separated using 12% SDS-PAGE and transferred to polyvinylidene difluoride membranes. Blots were incubated overnight with the primary antibodies against Bax (Cell Signaling Technology Danvers, MA, USA Cat# 5023S Lot# RRID: AB_10557411) and Cleaved Caspase-3 (Cell Signaling Technology Cat# 9661L Lot# RRID: AB_331441). After rinsing in TBST, the membranes were incubated with the HRP-conjugated secondary antibody (1:5000; ZSGB-Bio) for 1h. Bands were detected by chemiluminescence. Further, blots were stripped and re-probed with a GAPDH antibody (1:1000, GOOD HERE), thereby serving as a protein loading control. According to manufacturer's data sheet, Bax (D2E11) Rabbit mAb detects endogenous levels of total Bax protein at 20 kDa (single band). The Cleaved Caspase-3 (Asp175) Antibody of activated caspase-3 detects endogenous levels of the large fragment (17/19 kDa, two bands) of activated caspase-3 resulting from cleavage adjacent to Asp175. This antibody

does not recognize full length caspase-3 or other cleaved caspases. Band intensities were quantified using the Image J software (NIH). 4 mice were used for each group.

Immunohistochemistry

As a supplement for detecting the mitochondria apoptosis related proteins such as cytochrome c and APAF1, we also used immunohistochemistry. The animals were euthanized by intraperitoneal injection of 4% chloral hydrate and fixed with 4% paraformaldehyde. The cochlear specimens were placed in a refrigerator overnight at a 4°C and then decalcified with 10% EDTA for 7 days. The cochleae were dehydrated with 15% and 30% sucrose for 2–3 days until they sank to the bottom; then they were embedded with optimum cutting temperature (OCT) glue and sectioned into 5 μm thicknesses with cryomicrotome (Leica CM3050S, Nussloch, Germany). The sections were fixed by 4°C acetone for 20 min and then washed three times with 0.01M phosphate buffer solution (1×PBS) for 5 min each time. The samples were immersed in 0.1% Triton X-100 for 20 min, washed three times for 5 min with 1× PBS, submerged in 3% H_2O_2 for 20 min in the dark, and finally washed three times for 5 min with 1× PBS. Then, the samples were blocked with 5% goat serum at room temperature for 30 min. Anti-COX IV (Mitochondrial Marker) antibody (Abcam Cat# ab33985 Lot# RRID: AB_879754), anti-Cyt c antibody (Cytochrome c) (Cell Signaling Technology Cat# 4272 Lot# RRID: AB_2090454), and anti-APAF1 antibody (Abcam Cat# ab32372 Lot# RRID: AB_722822) were used as the primary antibodies and incubated at 4°C overnight. The next day, the samples were washed with 1× PBS three times for 5 min. Goat antimouse IgG (H+L) Alexa Fluor® 647 conjugate (1:200) and Goat antirabbit IgG (H+L) Alexa Fluor® 488 conjugate (1:200) were used as secondary antibodies and incubated for 40 minutes at 37°C temperature. The samples were washed three times for 5 min with 1× PBS. To label the nuclei, 4′, 6-diamidino-2-phenylindole (DAPI; Beyotime) was added to the samples for 5 min at room temperature before washing three times in PBS. The staining and image capture were performed as indicated above. 3 mice were used for each group.

Statistical Analysis

Data are expressed as mean ± SE, unless otherwise specified. SAS version 9.4 (SAS Institute, Inc.) proc mixed was used to perform a repeated measures analysis of variance for ABR thresholds and DPOAE data analysis. The difference between two groups for other measurements was determined by Unpaired Student t test using SPSS software (http://www-01.ibm.com/software/uk/analytics/spss/, RRID:SCR_002865); $p < 0.05$ was considered to be statistically significant.

Results

mNGF decreases the ABR thresholds in DBA/2J mice

ABR thresholds measurement is well accepted for hearing functional testing both in human and mice. The high frequencies such as 32 kHz represent the function of cochlear basal turn, the lower frequencies represent the function of cochlear epical turn. Normal mice have higher hearing sensitivity at 16 kHz–24 kHz. DBA/2J mice are well-known to have early-onset progressive hearing loss(Johnson et al. 2008). After daily treatments from 1 week of

age, ABR thresholds were measured at 5 weeks, 7 weeks, and 9 weeks of ages to click and to tone pips of 8, 16, and 32 kHz respectively. ABR thresholds in the mNGF group were significantly lower (10–15dB) than those in both the vehicle group and the non-treated group for high frequencies at the three time points (Fig. 2.B.), but not significantly lower for click and 8 kHz stimuli (Degrees of freedom =1, F=0.77, P>0.05, n=10, a repeated measures ANOVA with proc mixed, data not shown). Specifically, the ABR thresholds at the frequencies (Hz) of 16 kHz and 32 Hz were significantly (10–15dB) lower in the mNGF group than those in the vehicle group (Degrees of freedom =1, p<0.01, F = 50.54 and 34.45, n=10 for each frequency, a repeated measures ANOVA with proc mixed). Furthermore, in the vehicle group, the ABR thresholds at 9 weeks of age were significantly higher than those at 5 weeks of age at the frequency of 32kHz (Degrees of freedom =2, p<0.05, F 4.08, a repeated measures ANOVA with proc mixed), suggesting an aging effect. There were no significant interactions between age and treatment. (Degrees of freedom =2, F= 1.63, P>0.05, n=10, a repeated measures ANOVA with proc mixed). Given that a similar aging effect has been previously reported (Johnson et al. 2008) and that there is no difference between the vehicle group and the non-treated group, for the remainder of our analysis, we only compared mNGF groups and vehicle groups that were age-matched at each of the 3 time points with t-tests. For effect sizes, Cohen's d was calculated as the difference between the means divided by the pooled SD. The Effect Sizes for click and 8 kHz were between 0.09 and 0.46, except 0.67 for click at 7 weeks of age. In contrast, the Effect Sizes for 16 kHz and 32 kHz were between 1.06 and 2.08. There was no significant difference between male and female mice (data not shown). Therefore, for the rest of our experiments, we did not try to differentiate between genders.

mNGF increases DPOAE amplitudes in DBA/2J mice

DPOAE is another well-known hearing test for humans and mice, which is particularly recognized for testing the function of outer hair cells (OHCs). After testing the ABR threshold of each mouse, DPOAE was immediately measured. The level of DPOAE amplitudes in the mNGF group was generally 5–10 dB higher than that of the vehicle group at 5 and 7 weeks of ages (Fig. 2.D.) (P<0.01). Specifically, the DPOAE amplitude differences at the frequencies (Hz) of 6244, 8844, 12503, 17672, 24990 and 35344 were significantly higher in the mNGF group (Degrees of freedom =1, p<0.01 F values 41.31, 20.04, 19.37, 35.78, 43.07, 9.98 for each of them respectively, n=10, a repeated measures ANOVA with proc mixed) (Fig. 2.C, D). Furthermore, the difference in mNGF effect among those at 7 weeks of age was significantly higher than the difference in mNGF effect among those at 9 weeks of age, particularly at higher frequencies of 17672 Hz, (Degrees of freedom =2, F= 3.83, P<0.05), 24990Hz, (Degrees of freedom =2, F=12.78, P<0.01), 35344Hz (Degrees of freedom =2, F=9.56 P<0.05, a repeated measures ANOVA with proc mixed) (Fig. 2.D). These data indicate that the mNGF protected the functions of the OHCs in DBA/2J mice with highest effect at 7 weeks of age at 24990Hz. Cohen's d at 24990Hz was the highest at 2.70 in contrast to all other significant Cohen's d values ranging between 0.94 and 1.80. The 24990Hz DPOAE represents the OHCs' function at the most sensitive frequency of hearing for mice (Muller et al. 2005).

Histological examination revealed mNGF protects stria vascularis, spiral ganglion neurons, and hair cells in the cochlea of DBA/2J mice

We compared morphological changes in these cochlear structures caused by mNGF treatment to changes observed in the vehicle group at corresponding hearing testing ages. Lesions of the hair cells and SGNs were presented as OHC and neuronal cell loss, while stria vascularis was present as width changes. Morphological changes between the groups at the three time points are shown in Fig. 3.A. OHC loss was obvious at the age of 9 weeks, and the mNGF-treated group presented less cell loss than the vehicle group. At the other two time points, there is no significant difference between the two groups.

The survival of SGNs in the basal cochlear regions was calculated (Fig. 3.C). The protective effects of mNGF on SGNs at earlier ages (5 weeks and 7 weeks) were significant ($p<0.05$, $n=5$) and stronger than those at the later age (9 weeks).

The widths of stria vascularis in the mNGF group were thicker than those of the vehicle group (Fig. 3.A and B), but only to a significant degree at 9 weeks of age ($p<0.01$, $n=5$).

OHCs were stained with Alexa Fluor 488 conjugated to phalloidin (Fig. 3.D). OHC loss was counted; the percentages of OHC loss in the cochleae at the three time points are shown in Fig. 3.E. There was barely any OHC loss at the apex and middle turns of the cochleae at the three time points (data not shown). However, loss of OHCs was significantly less in the basal turns of cochleae in the mNGF-treated group compared to that of the vehicle group at 9 weeks of age ($p<0.01$; $n=5$,).

mNGF inhibits apoptosis of spiral ganglion neuron cells in DBA/2J mice

Hearing loss is usually accompanied by SGN apoptosis. mNGF-treated mice showed fewer TUNEL-positive cells (Fig. 4.A) than the vehicle group at the three time points. Quantification and statistical analysis of the TUNEL staining showed that the number of TUNEL-positive cells decreased significantly in the mNGF-treated group compared to the vehicle group ($p<0.01$, $n=4$) (Fig. 4.B).

mNGF treatment down-regulates apoptosis-related genes in the cochleae of DBA/2J mice

Apoptosis may play a potential role in the early onset of hearing loss (Yang et al. 2015). Gene expression profiles in the inner ears of DBA/2J mice at 5, 7, and 9 weeks of age were detected simultaneously in the mNGF-treated and vehicle groups. The results demonstrated that apoptosis-related genes, such as *Bak*, *Bax*, *Caspase-9*, and *Caspase-3*, were down-regulated in the mNGF-treated group at the three time points (Fig. 5). The mRNA levels of *Bak* and *Bax*, which are taken from the mitochondrial membrane, were significantly lower in the mNGF-treated group compared to the vehicle group at the 5th and 7th weeks (Fig. 5.A, B) ($p<0.05$) respectively, but not at the 9th week. However, the expression of *Caspase-9* and *Caspase 3* was significantly down-regulated in the mNGF-treated group at 9 weeks of age compared to the vehicle group (Fig. 5.C) ($p<0.05$). The results indicate that mNGF might down-regulate apoptosis-related genes to slow hearing loss in DBA/2J mice.

mNGF treatment down-regulates the expression of apoptosis-related proteins in cochlea

Western blotting data in the present study indicated that mNGF treatment decreased apoptosis-related protein expression in the cochlea to protect hearing (Fig. 6.A and B). The apoptosis-related proteins *Bax* and *Caspase-3* in the mNGF-treated group showed lower expression than the vehicle group at 7 weeks of age, and *Bax* at 9 weeks of age; however, there was no significant difference at 5 weeks of age. Quantification and statistical analysis of the relative intensity fold by Western blotting showed that the levels of *Bax* and *Caspase-3* expression in the mNGF-treated group were lower than in the vehicle group (Fig. 6.C and D). Cytochrome c is released from the mitochondria and plays a critical step in the apoptotic cascade (Bouchier-Hayes et al. 2008). The level of cytochrome c decreases in the mitochondrial fraction and increases in the cytosolic fraction when apoptosis occurs (Yan et al. 2015). In our study, we observed that cytochrome c in the mitochondria achieved greater expression in the mNGF-treated mice than the vehicle mice at the three time points (Fig. 6.E). Furthermore, immunostaining showed that the expressed level of APAF1 in the SGNs of basal turns was much higher in the vehicle group than in the mNGF-treated group (Fig. 6.F). APAF1 plays an essential role in apoptosis. In the presence of cytochrome c and dATP, APAF1 assembles into an oligomeric apoptosome and is responsible for the activation of procaspase-9 and the maintenance of the enzymatic activity of processed caspase-9 (Bao et al. 2007).

Discussion

mNGF ameliorate ePHL and related cochlear pathology in DBA/2J mice

In present study, we used DBA/2J mice to evaluate the otoprotective effects of mNGF and determined that mNGF could preserve hearing and maintain the function of OHCs in DBA/2J mice (Fig. 2). These results were further supported by less OHC and SGNs loss and less inhibited SV degeneration in mNGF-treated cochleae compared to vehicle cochleae of DBA/2J mice (Fig. 3). Thus, the otoprotective effects of mNGF against PHL in DBA/2J mice were demonstrated. The mNGF treatments were started at 7 days of age with the mice, but in our experience, ABR thresholds and DPOAE can only be accurately measured after 20 days of age. Thus we could not have performed pre-treatment testing before 7 days of age. Previous studies suggested that DBA/2J mice displayed early-onset AHL at about 3–4 weeks of age. As previously reported, the mean ABR thresholds for DBA/2J mice at 3 weeks for click, 8kHz, 16Hz, and 32 kHz were 43±4, 28±4, 28±18 and 53±12 dB SPL, while the mean thresholds for CBA/CaJ mice (a well-recognized normal hearing strain) at 9–39 weeks were 36, 24, 15, and 39 dB SPL for the click, 8 kHz, 16 kHz, and 32 kHz stimuli, respectively (Zheng et al. 1999). Our data showed (Figure 2B) that the ABR thresholds of the mNGF group at 5 and 7 weeks are quite similar to the normal values at 32 kHz in this literature. The ABR is a far field evoked potential consisting of several peaks (I–V) representing activation of specific generators along the auditory pathway from the cochlea to the brainstem via the auditory nerve. The long-lasting effect of mNGF on ABR thresholds (Fig. 2A and B) from 5–9 weeks of age may result from its effect on the pathological changes in different cochlear structures that occur at various time points. For example, at 9 weeks of age, SGN may have the highest deterioration rate, whereas at this age mNGF showed a more significant effect on ABR thresholds. The treatment was terminated

at 9 weeks of age because DPOAE showed that the beneficial effects of mNGF had decreased comparing to the 7 weeks' data. DPOAE, measuring OHC's function, may reflect the highest functional deterioration rate at around 7 weeks of age in the vehicle group, thus indicating the best window of time for the mNGF therapy. The hair cell counts in Fig. 3A seem to differ from Fig. 3D; however, upon closer examination, one can clearly see that there is no hair cell loss in Fig. 3A at 5 or 7 weeks because a section missed or displaced the nucleus of normal hair cells. In contrast, SGN damage is already severe at 5 weeks of age and thus mNGF treatment effectively rescued the SGNs (Fig. 3A and C) and ABR thresholds (Fig. 2A and B) at this age. The therapeutic effect of mNGF on SGN is stronger and earlier than its effect on the OHCs. The OHC damage mostly affected the basal turn of the cochlear, which is responsible for high frequency detection. This data provides a good explanation of why mNGF had the best effect on high frequency hearing loss (Muller et al. 2005). These data provide morphological and functional evidence that mNGF can prevent hearing loss in an animal model. Although we expected the male mice to have more severe hearing loss as well as a better response to the treatment (because men have significantly faster rates of threshold increase than women (Kim et al. 2010)), our data did not find a gender difference in either hearing loss or mNGF effect.

However, therapeutic use of human NGF is limited due to the blood–brain barrier (BBB). NGF is able to cross the BBB under specific conditions, such as when the BBB has been damaged. In this paper, we observed some minor stria vascularis damage in the DBA/2J mice (Fig. 3), which may have increased the penetration of mNGF across the blood–labyrinth barrier. In previous studies on animal models for neurotrophic treatment of hair cell loss, the treatment was mostly delivered using local drug delivery to the inner ears. But in those studies, it had a significant hearing-protective effect in noise-induced hearing loss (Shoji et al. 2000) and drug-induced hair cell loss (Ruan et al. 1999). Recently, a randomized, controlled clinical trial of the topical insulin-like growth factor-1 (IGF-1) therapy in patients with sudden sensorineural hearing loss (SSHL) was performed and compared to intratympanic corticosteroid therapy. The positive effect of the topical IGF-1 application on hearing levels and its favorable safety profile suggest topical IGF-1 therapy as a salvage treatment for SSHL (Nakagawa et al. 2014). In order to reduce systematic adverse effects, this study was performed using a topical IGF-1 application. Our study did not observe any systematic adverse effects over a 8-week period. In another study on deaf guinea pigs, the long-term effects of temporary treatment with brain-derived neurotrophic factor (BDNF) showed that, after treatment cessation, the neuroprotective effect continued for at least 8 weeks (Ramekers et al. 2015). Although we did not study the long-term effects of mNGF, it deserves further study.

mNGF preventing hearing loss via suppression of apoptosis pathway

The molecular mechanisms underlying hearing loss are largely unknown. It is very difficult to evaluate any prophylactic efficacy of a drug and to investigate the molecular mechanisms underlying hearing loss on human patients. An alternate and complementary approach to these human studies is using mouse models (Ohmen et al. 2014). Inbred mouse strains serve as important models for hearing loss. DBA/2J mice have homozygous mutations in *Cdh23*$^{ahl/ahl}$ and *Fscn2*$^{ahl8/ahl8}$ as well as other quantitative trait loci (QTLs) that modify the

severity of hearing loss (Johnson et al. 2015). Recently, our data and the data of others show that mutations of *Cdh23* gene can cause apoptosis in the inner ear (Han et al. 2012). Apoptosis in the cochleae is widely understood to contribute to PHL (Dirks et al. 2006; Kujoth et al. 2007; Someya and Prolla 2010; Yamasoba et al. 2013). There are mainly two pathways that trigger apoptosis: the intrinsic pathway and the extrinsic pathway (Youle and Strasser 2008). The former is also known as the mitochondrial pathway (Fig. 7), which is a Bak-dependent pathway and may be involved in the cochlear aging in DBA/2J mice (Someya et al. 2009). By administering mNGF to DBA/2J mice in our study, we verified that apoptosis-related genes, especially *Bak*, *Bax*, and *Caspase-3*, were generally less expressed in mNGF-treated mice compared to control mice but varied reasonably between mRNA (Fig. 5) and/or protein (Fig. 6) levels. There are multiple post-transcriptional mechanisms involved in protein modification, such as the activation of cleaved Caspase-3 protein. Additionally, there is no significant effect of mGNF on Bak and Bax at 9 weeks, in contrast to its effect at 5 and 7 weeks. A possible explanation is that the number of mitochondria markedly decreases at 9 weeks of age. TUNEL-positive cells in mNGF-treated mice were lower than in the vehicle group at the three time points tested (Fig. 4B). These results further elucidated the apoptosis mechanisms underlying the hearing loss in DBA/2J mice.

NGF can promote neuronal survival and growth mainly by binding with TrkA receptors and $p75^{NTR}$ receptors on cell surfaces. B-cell lymphoma-extra large (*Bcl-xL*) is one of the prosurvival members of the Bcl-2 family, which can rescue SGNs deprived of trophic factor in vitro and in vivo (Hansen et al. 2007). The combination of NGF and TrkA can cause Bcl-2 to be highly expressed and, thus, eventually prevent apoptosis (Sofroniew et al. 2001). mNGF—which shares a nearly 90% homologous amino acid sequence with the NGF of humans and also plays an important regulating role in neuron survival, growth, differentiation, and maintenance (Apfel et al. 1998; Bibel and Barde 2000; Verge et al. 1996)—may provide a new therapeutic modality for hearing loss. In the present study, the otoprotective effects of mNGF were confirmed. We found that the otoprotective effects of mNGF were strongest at 7 weeks of age by using DPOAE (Fig. 2C and D). Moreover, the difference in the expression level of *caspase-3* at 7 weeks of age was the most obvious compared to the other two time points with Western blotting (Fig. 6D). Therefore, we suppose that the most effective time for mNGF treatment in DBA/2J mice is at about 7 weeks. As the most common exogenous form of NGF, mNGF has been produced commercially in China. We adopted the manufacturer-recommended dose for injection of mNGF. More importantly, no abnormal activities have been observed in the treated mice for up to 8 weeks of treatment, indicating no serious side effects from mNGF injection.

In summary, our data support our hypothesis that mNGF has significant otoprotective effect in PHL of DBA/2J mice. mNGF can attenuate cochlear cell death through the Bak-dependent mitochondrial apoptosis pathways.

Acknowledgments

Contract grant sponsor: National Institutes of Health; grant R01DC015111; the Taishan Scholar Program; Natural Science Foundation of Shandong Province; Contract grant sponsor: ZR2012HL30, ZR2014HL050; National Natural Science Foundation of China (NSFC): 81271085, 81530030, 81500797, and 81400467.

We thank Dr. Oumei Wang, Dr. Shuang Shen, and Dr. Liyan Bi for experimental guidance, Drs. Tianhe Xu and Dr. Chuan-Ming Li for statistical advice. This study was supported by the National Institutes of Health (R01DC015111), the Taishan Scholar Program, the Natural Science Foundation of Shandong Province (ZR2012HL30, ZR2014HL050), and the National Natural Science Foundation of China (81271085, 81530030, 81500797, and 81400467).

References

Angeli S, Lin X, Liu XZ. Genetics of hearing and deafness. Anat Rec (Hoboken). 2012; 295(11): 1812–1829. [PubMed: 23044516]

Apfel SC, Kessler JA, Adornato BT, Litchy WJ, Sanders C, Rask CA. Recombinant human nerve growth factor in the treatment of diabetic polyneuropathy. NGF Study Group. Neurology. 1998; 51(3):695–702. [PubMed: 9748012]

Bao Q, Lu W, Rabinowitz JD, Shi Y. Calcium blocks formation of apoptosome by preventing nucleotide exchange in Apaf-1. Molecular cell. 2007; 25(2):181–192. [PubMed: 17244527]

Bernd P, Represa J. Characterization and localization of nerve growth factor receptors in the embryonic otic vesicle and cochleovestibular ganglion. Dev Biol. 1989; 134(1):11–20. [PubMed: 2543603]

Bibel M, Barde YA. Neurotrophins: key regulators of cell fate and cell shape in the vertebrate nervous system. Genes Dev. 2000; 14(23):2919–2937. [PubMed: 11114882]

Bothwell M. Functional interactions of neurotrophins and neurotrophin receptors. Annu Rev Neurosci. 1995; 18:223–253. [PubMed: 7605062]

Bouchier-Hayes L, Munoz-Pinedo C, Connell S, Green DR. Measuring apoptosis at the single cell level. Methods. 2008; 44(3):222–228. [PubMed: 18314052]

Datta SR, Dudek H, Tao X, Masters S, Fu H, Gotoh Y, Greenberg ME. Akt phosphorylation of BAD couples survival signals to the cell-intrinsic death machinery. Cell. 1997; 91(2):231–241. [PubMed: 9346240]

del Peso L, Gonzalez-Garcia M, Page C, Herrera R, Nunez G. Interleukin-3-induced phosphorylation of BAD through the protein kinase Akt. Science. 1997; 278(5338):687–689. [PubMed: 9381178]

Despres G, Hafidi A, Romand R. Immunohistochemical localization of nerve growth factor receptor in the cochlea and in the brainstem of the perinatal rat. Hear Res. 1991; 52(1):157–165. [PubMed: 1648058]

Dirks AJ, Hofer T, Marzetti E, Pahor M, Leeuwenburgh C. Mitochondrial DNA mutations, energy metabolism and apoptosis in aging muscle. Ageing Res Rev. 2006; 5(2):179–195. [PubMed: 16647308]

Doerks T, Copley RR, Schultz J, Ponting CP, Bork P. Systematic identification of novel protein domain families associated with nuclear functions. Genome Res. 2002; 12(1):47–56. [PubMed: 11779830]

Greene LA, Kaplan DR. Early events in neurotrophin signalling via Trk and p75 receptors. Curr Opin Neurobiol. 1995; 5(5):579–587. [PubMed: 8580709]

Han F, Yu H, Tian C, Chen HE, Benedict-Alderfer C, Zheng Y, Wang Q, Han X, Zheng QY. A new mouse mutant of the Cdh23 gene with early-onset hearing loss facilitates evaluation of otoprotection drugs. Pharmacogenomics J. 2012; 12(1):30–44. [PubMed: 20644563]

Han F, Yu H, Zheng T, Ma X, Zhao X, Li P, Le L, Su Y, Zheng QY. Otoprotective effects of erythropoietin on Cdh23erl/erl mice. Neuroscience. 2013; 237:1–6. [PubMed: 23384607]

Hansen MR, Roehm PC, Xu N, Green SH. Overexpression of Bcl-2 or Bcl-xL prevents spiral ganglion neuron death and inhibits neurite growth. Developmental neurobiology. 2007; 67(3):316–325. [PubMed: 17443790]

Hantzopoulos PA, Suri C, Glass DJ, Goldfarb MP, Yancopoulos GD. The low affinity NGF receptor, p75, can collaborate with each of the Trks to potentiate functional responses to the neurotrophins. Neuron. 1994; 13(1):187–201. [PubMed: 8043276]

Huang EJ, Reichardt LF. Trk receptors: roles in neuronal signal transduction. Annual review of biochemistry. 2003; 72:609–642.

Johnson KR, Longo-Guess C, Gagnon LH, Yu H, Zheng QY. A locus on distal chromosome 11 (ahl8) and its interaction with Cdh23 ahl underlie the early onset, age-related hearing loss of DBA/2J mice. Genomics. 2008; 92(4):219–225. [PubMed: 18662770]

Johnson KR, Longo-Guess CM, Gagnon LH. A QTL on Chr 5 modifies hearing loss associated with the fascin-2 variant of DBA/2J mice. Mammalian genome: official journal of the International Mammalian Genome Society. 2015; 26(7–8):338–347. [PubMed: 26092689]

Kim S, Lim EJ, Kim HS, Park JH, Jarng SS, Lee SH. Sex Differences in a Cross Sectional Study of Age-related Hearing Loss in Korean. Clin Exp Otorhinolaryngol. 2010; 3(1):27–31. [PubMed: 20379399]

Kujoth GC, Bradshaw PC, Haroon S, Prolla TA. The role of mitochondrial DNA mutations in mammalian aging. PLoS Genet. 2007; 3(2):e24. [PubMed: 17319745]

Muller M, von Hunerbein K, Hoidis S, Smolders JW. A physiological place-frequency map of the cochlea in the CBA/J mouse. Hear Res. 2005; 202(1–2):63–73. [PubMed: 15811700]

Nakagawa T, Kumakawa K, Usami S, Hato N, Tabuchi K, Takahashi M, Fujiwara K, Sasaki A, Komune S, Sakamoto T, Hiraumi H, Yamamoto N, Tanaka S, Tada H, Yamamoto M, Yonezawa A, Ito-Ihara T, Ikeda T, Shimizu A, Tabata Y, Ito J. A randomized controlled clinical trial of topical insulin-like growth factor-1 therapy for sudden deafness refractory to systemic corticosteroid treatment. BMC Med. 2014; 12:219. [PubMed: 25406953]

Ohmen J, Kang EY, Li X, Joo JW, Hormozdiari F, Zheng QY, Davis RC, Lusis AJ, Eskin E, Friedman RA. Genome-wide association study for age-related hearing loss (AHL) in the mouse: a meta-analysis. J Assoc Res Otolaryngol. 2014; 15(3):335–352. [PubMed: 24570207]

Park JB, Lee CK, Koh JS, Lee JK, Park EY, Riew KD. Overexpressions of nerve growth factor and its tropomyosin-related kinase A receptor on chordoma cells. Spine (Phila Pa 1976). 2007; 32(18): 1969–1973. [PubMed: 17700442]

Polak M, Eshraghi AA, Nehme O, Ahsan S, Guzman J, Delgado RE, He J, Telischi FF, Balkany TJ, Van De Water TR. Evaluation of hearing and auditory nerve function by combining ABR, DPOAE and eABR tests into a single recording session. J Neurosci Methods. 2004; 134(2):141–149. [PubMed: 15003380]

Raimundo N, Song L, Shutt TE, McKay SE, Cotney J, Guan MX, Gilliland TC, Hohuan D, Santos-Sacchi J, Shadel GS. Mitochondrial stress engages E2F1 apoptotic signaling to cause deafness. Cell. 2012; 148(4):716–726. [PubMed: 22341444]

Ramekers D, Versnel H, Strahl SB, Klis SF, Grolman W. Temporary Neurotrophin Treatment Prevents Deafness-Induced Auditory Nerve Degeneration and Preserves Function. J Neurosci. 2015; 35(36):12331–12345. [PubMed: 26354903]

Ruan RS, Leong SK, Mark I, Yeoh KH. Effects of BDNF and NT-3 on hair cell survival in guinea pig cochlea damaged by kanamycin treatment. Neuroreport. 1999; 10(10):2067–2071. [PubMed: 10424676]

Semaan MT, Zheng QY, Han F, Zheng Y, Yu H, Heaphy JC, Megerian CA. Characterization of neuronal cell death in the spiral ganglia of a mouse model of endolymphatic hydrops. Otol Neurotol. 2013; 34(3):559–569. [PubMed: 23462289]

Shin JB, Longo-Guess CM, Gagnon LH, Saylor KW, Dumont RA, Spinelli KJ, Pagana JM, Wilmarth PA, David LL, Gillespie PG, Johnson KR. The R109H variant of fascin-2, a developmentally regulated actin crosslinker in hair-cell stereocilia, underlies early-onset hearing loss of DBA/2J mice. The Journal of neuroscience: the official journal of the Society for Neuroscience. 2010; 30(29):9683–9694. [PubMed: 20660251]

Shoji F, Miller AL, Mitchell A, Yamasoba T, Altschuler RA, Miller JM. Differential protective effects of neurotrophins in the attenuation of noise-induced hair cell loss. Hear Res. 2000; 146(1–2):134–142. [PubMed: 10913890]

Sofroniew MV, Howe CL, Mobley WC. Nerve growth factor signaling, neuroprotection, and neural repair. Annu Rev Neurosci. 2001; 24:1217–1281. [PubMed: 11520933]

Someya S, Prolla TA. Mitochondrial oxidative damage and apoptosis in age-related hearing loss. Mech Ageing Dev. 2010; 131(7–8):480–486. [PubMed: 20434479]

Someya S, Xu J, Kondo K, Ding D, Salvi RJ, Yamasoba T, Rabinovitch PS, Weindruch R, Leeuwenburgh C, Tanokura M, Prolla TA. Age-related hearing loss in C57BL/6J mice is mediated by Bak-dependent mitochondrial apoptosis. Proc Natl Acad Sci U S A. 2009; 106(46):19432–19437. [PubMed: 19901338]

Verge VM, Gratto KA, Karchewski LA, Richardson PM. Neurotrophins and nerve injury in the adult. Philos Trans R Soc Lond B Biol Sci. 1996; 351(1338):423–430. [PubMed: 8730781]

Yamasoba T, Lin FR, Someya S, Kashio A, Sakamoto T, Kondo K. Current concepts in age-related hearing loss: epidemiology and mechanistic pathways. Hear Res. 2013; 303:30–38. [PubMed: 23422312]

Yan X, Jiang Z, Bi L, Yang Y, Chen W. Salvianolic acid A attenuates TNF-alpha- and D-GalN-induced ER stress-mediated and mitochondrial-dependent apoptosis by modulating Bax/Bcl-2 ratio and calcium release in hepatocyte LO2 cells. Naunyn Schmiedebergs Arch Pharmacol. 2015; 388(8): 817–830. [PubMed: 25943027]

Yang L, Zhang H, Han X, Zhao X, Hu F, Li P, Xie G, Gao L, Cheng L, Song X, Han F. Attenuation of hearing loss in DBA/2J mice by anti-apoptotic treatment. Hear Res. 2015; 327:109–116. [PubMed: 26003529]

Youle RJ, Strasser A. The BCL-2 protein family: opposing activities that mediate cell death. Nat Rev Mol Cell Biol. 2008; 9(1):47–59. [PubMed: 18097445]

Zhang X, Zheng T, Sang L, Apisa L, Zhao H, Fu F, Wang Q, Wang Y, Zheng Q. Otitis media induced by peptidoglycan-polysaccharide (PGPS) in TLR2-deficient (Tlr2(−/−)) mice for developing drug therapy. Infect Genet Evol. 2015; 35:194–203. [PubMed: 26296608]

Zheng QY, Ding D, Yu H, Salvi RJ, Johnson KR. A locus on distal chromosome 10 (ahl4) affecting age-related hearing loss in A/J mice. Neurobiology of aging. 2009; 30(10):1693–1705. [PubMed: 18280008]

Zheng QY, Johnson KR, Erway LC. Assessment of hearing in 80 inbred strains of mice by ABR threshold analyses. Hear Res. 1999; 130(1–2):94–107. [PubMed: 10320101]

Significance Statement

Most progressive hearing loss that results from sensorineural damage is irreversible and currently has no proven cure. Nerve growth factor (NGF) has been studied extensively for promoting neuronal survival and growth. However, we do not know its otoprotective effect in progressive hearing loss (PHL). Here, we show that mouse nerve growth factor (mNGF) can attenuate hearing loss through the Bak-dependent mitochondrial apoptosis. Our findings suggest that mNGF can provide a new mode for ameliorating hearing loss and act as an otoprotectant for AHL.

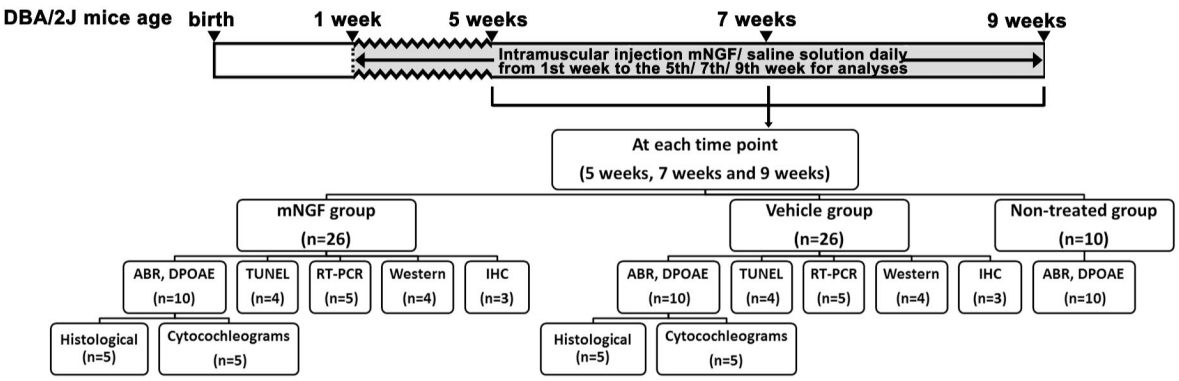

Figure 1.

Workflow of the experiments. A total of 186 DBA/2J mice aged 1 week were divided into the mNGF-treated group (n=78), the vehicle group (n=78), and the non-treated group (n=30). To determine whether mNGF could ameliorate progressive hearing loss (PHL) in DBA/2J mice, saline or mNGF (saline solution, 64.8 μg/kg) was administered to DBA/2J mice of either sex by daily intramuscular injection from the 1st to the 9th week after birth. At 5, 7, and 9 weeks of age, auditory-evoked brainstem response (ABR) thresholds and distortion product oto-acoustic emission (DPOAE) were measured by a person blind to the treatments in the mNGF-treated group, the vehicle group, and the non-treated group (male 5, female 5, n=10 for each group). After ABR and DPOAE hearing measurements were taken, the same mice in the mNGF-treated group and the vehicle group were euthanized by intraperitoneal injection of 4% chloral hydrate to perform histological analyses (n=5) and cytocochleograms (n=5). Other mice in the mNGF-treated group and the vehicle group were also euthanized to conduct TUNEL staining (n=4), real time PCR (n=5), and western blotting (n=4) or Immunohistochemistry (n=3) analyses.

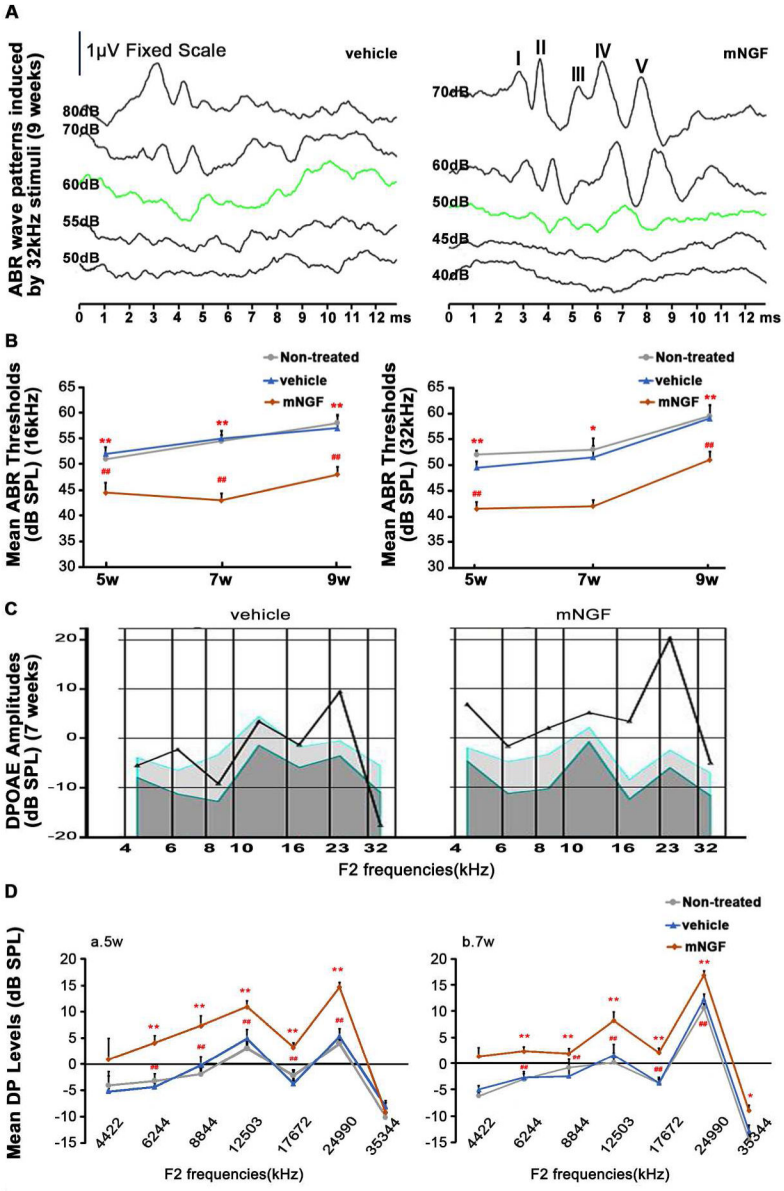

Figure 2.

Characterization of hearing loss in DBA/2J mice and mNGF effect through time course observation. (A): Determination of ABR thresholds. ABR wave patterns for 9 week old DBA/2J mice of vehicle group induced by 32kHz stimuli of 80, 70, 60, 55 and 50 dB SPL. Onset of stimulus is at 0 ms. A half cosine square window was used to create tone burst signals with a 3 ms duration. The ABR threshold for this mouse was estimated to be 60 dB SPL. ABR wave patterns for a 9-week-old DBA/2J mice of mNGF group induced by 32kHz stimuli of 70, 60, 50, 45, and 40 dB SPL. The ABR threshold for this mouse was estimated to be 50 dB SPL. Green line indicates threshold (dB SPL). (B) ABR thresholds in DBA/2J mice repeatedly detected at 5, 7, and 9 weeks of age (male 5, female 5, n=10 for each group). Error bars: standard error of the mean. The results show that ABR thresholds at high frequency were significantly lower in the mNGF-treated mice than those of the vehicle

group and non-treated mice at the three time points ($p<0.01$). No significant difference was found between the saline-treated groups and non-treated groups or between male and female mice. (C): The mNGF-treated mouse presented DPOAE amplitudes much higher than the saline-treated mice at 7 weeks of age. (D) DPOAE in DBA/2J mice measured at 5and 7 weeks of age (n=10). DPOAE amplitudes were significantly higher in the mNGF-treated mice than in those of the saline-treated mice and non-treated mice at the two time points, Error bars: standard error of the mean. The saline-treated groups and non-treated groups had no statistically significant difference ($p>0.05$). w, weeks; *indicate vehicle group and mNGF-treated group are statistically significant different ($p<0.05$); ** mean vehicle group and mNGF-treated group have a statistically significant difference ($p<0.01$), ABR, auditory-evoked brainstem response; DPOAE, distortion product otoacoustic emission; SPL, sound pressure level.

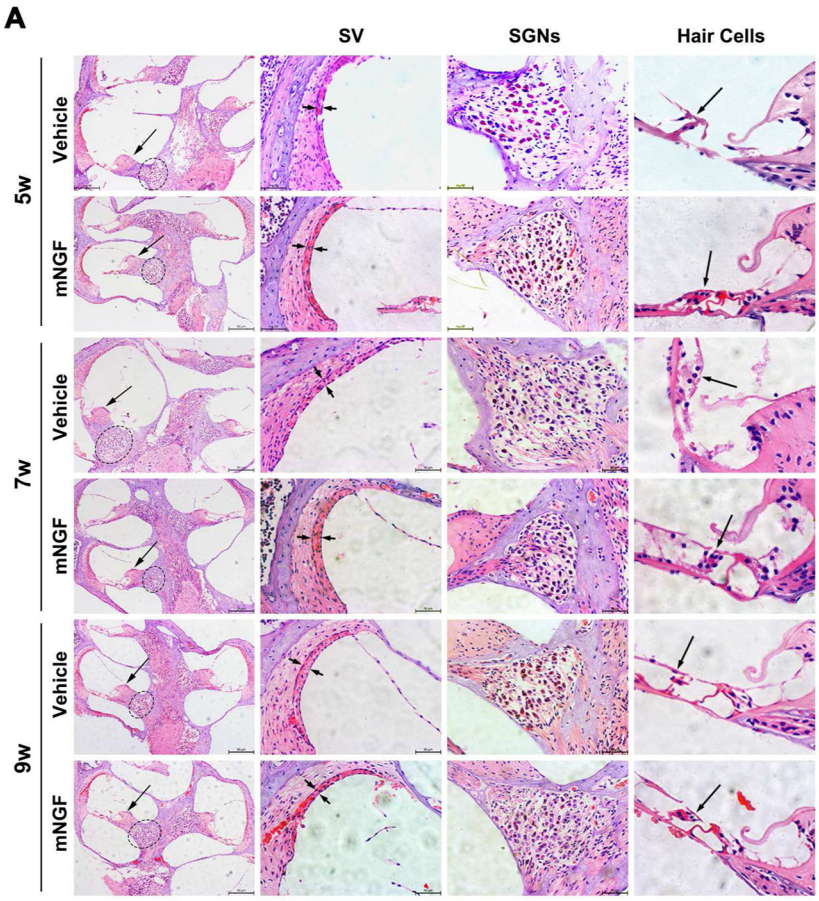

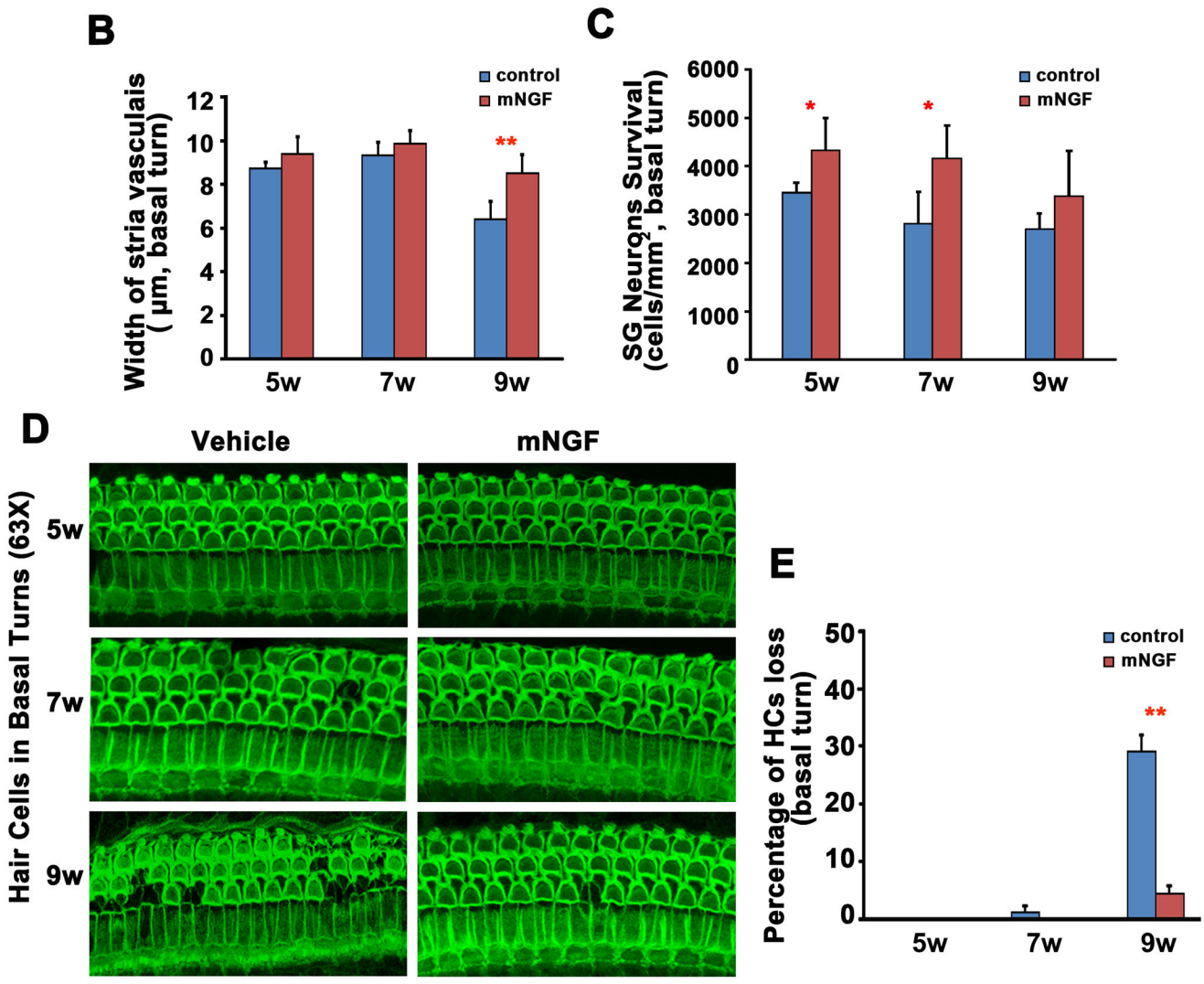

Figure 3. Pathological features of DBA/2J mice at 5 weeks, 7 weeks, and 9 weeks in the vehicle group and the group treated by mNGF, respectively

(A) Loss of outer hair cells, SGNs, and the thickness of stria vascularis in the basal turns of cochleae were observed by HE staining. Scale bar=50 μm.

(B) The width of stria vascularis. The mean width of stria vascularis in the basal cochlear regions of the mNGF-treated mice was generally thicker than that of the saline-treated mice, especially in the 9-week-olds. **Significantly different between the two groups at the time point ($p<0.01$, n=5). Error bars represent the SD from the mean.

(C) SG neuron survival (i.e., SG neuron density). The mean SGN density of the basal cochlear regions of the mNGF-treated mice was significantly higher than that of the saline-treated mice at the three time points, especially at 5 and 7 weeks. *Significantly different between the two groups at each time point ($p<0.05$, n=5). Error bars represent the SD from the mean.

(D) The loss of OHCs in the basal turns of the cochleae was observed under confocal microscope. Surface prepared basilar membranes were stained with alexa-fluor-488-

phalloidin. OHC loss occurred at 9 weeks old, but no significant OHC loss could be observed at other time points; the difference between mNGF-treated and vehicle groups at 9 weeks was significant. OHC, outer hair cell; scale bars=50 μm.

(E) Percentage of OHC loss in cochleae at three time points. The loss of OHC was significantly decreased at the basal turns of cochleae in the mNGF-treated group compared to that in the vehicle group at 9 weeks of age. *$p<0.05$, **$p<0.01$; n=5 at each time point; w, weeks.

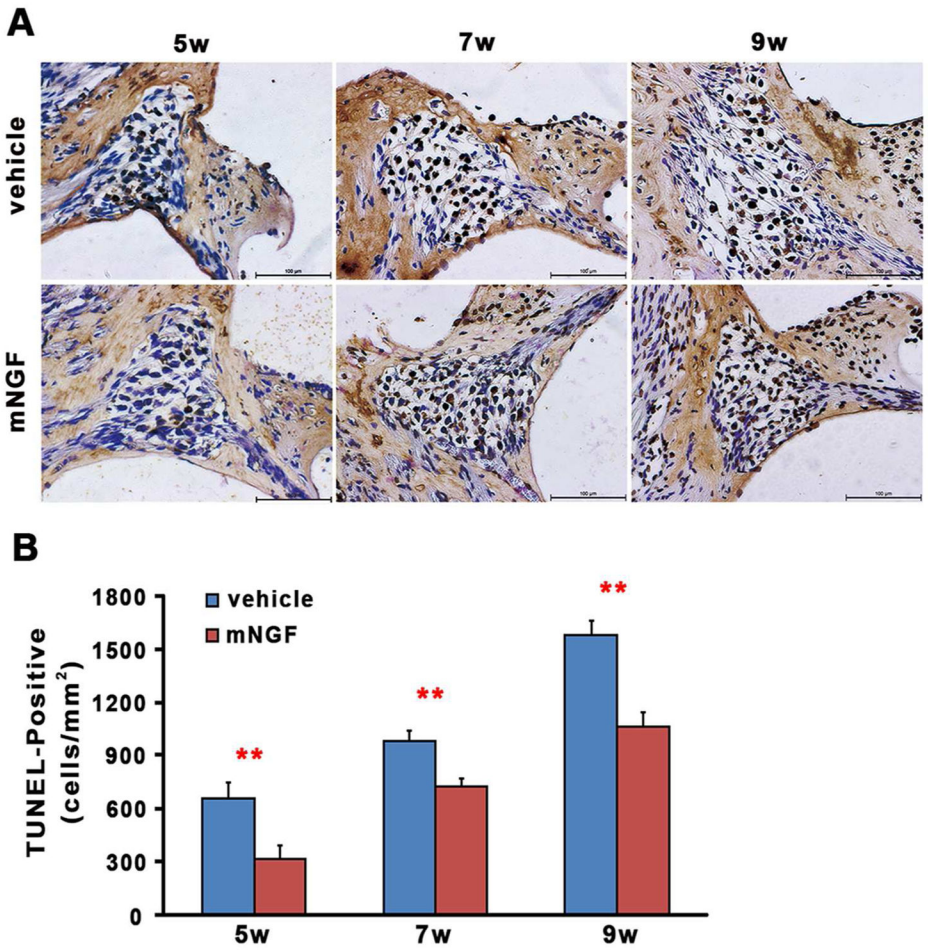

Figure 4.

Apoptosis features measured by TUNEL staining. (A) Representative photomicrographs of TUNEL staining in the basal turn from 5-, 7-, and 9-week-old DBA/2J mice, respectively, from vehicle and mNGF groups. Scale bar=100 μm. (B) TUNEL-positive cells were counted in the cochlea of mNGF-treated and vehicle mice at 5, 7, and 9 weeks of age. n=4. **Significantly different between the mNGF-treated and vehicle groups ($p<0.01$). Error bars represented as mean±SD. **$p<0.01$.

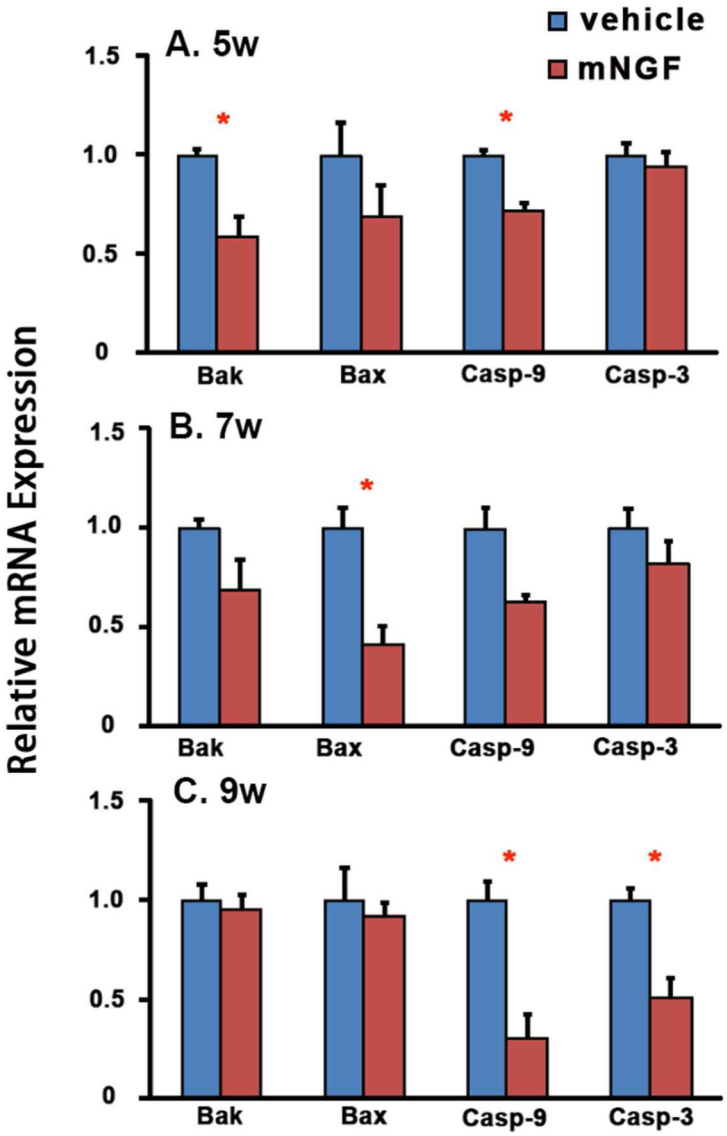

Figure 5.

Relative mRNA levels of apoptosis-related genes in the cochleae of DBA/2J mice. Bak, Bax, Caspase-9, and Caspase-3 levels were significantly lower in the inner ears of mNGF-treated mice than those in saline-treated mice. (A) Relative mRNA levels of DBA/2J mice at 5 weeks old, with treatment for 4 weeks. The levels of Bak and Caspase-9 were significantly lower than in the vehicle group. (B) The Bax level showed an obvious difference at 7 weeks. (C) The level of Caspase-9 and Caspase-3 was significantly lower after treatment for 8 weeks. n=5. Error bars represent the SD from the mean. *$p<0.05$.

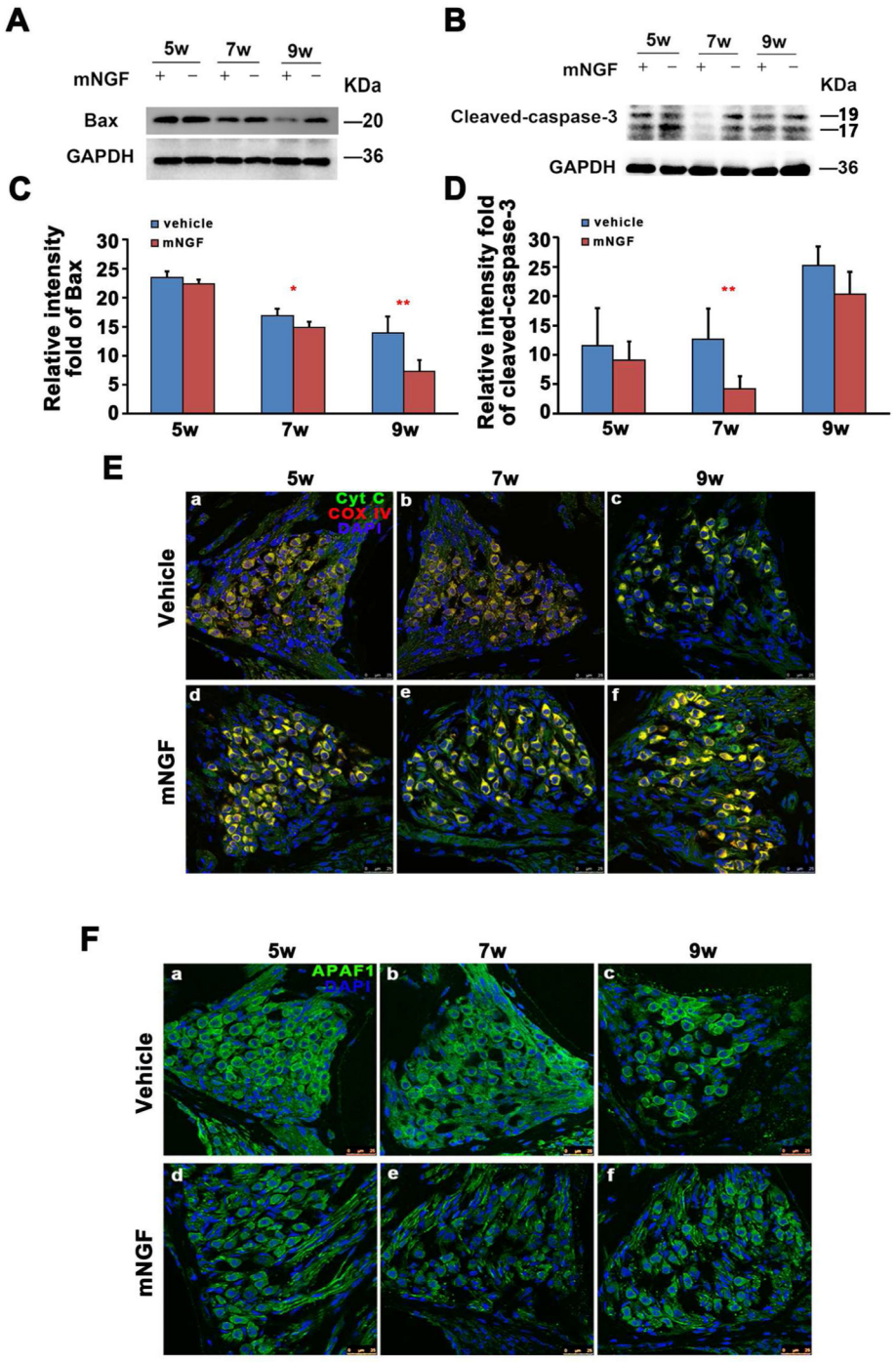

Figure 6. The indicated protein levels in mitochondrial pathway apoptosis in DBA/2J mice were determined by Western blotting

(A and B) Western blot of Bax (20 kDa) and cleaved Caspase-3 (17/19 kDa) in vehicle and mNGF groups' cochleae at three time points using GAPDH (36 kDa) as the loading control. (C and D) The average gray intensity of Bax and cleaved Caspase-3 proteins detected by Western blotting was standardized to that of GAPDH. n=4, Values are expressed as mean ±SD; *p<0.05, **p<0.01.

(E) Immunostaining for Cyt C in mitochondrion of SGNs in the basal turns of cochleae in DBA/2J mice aged 5, 7, and 9 weeks. Stronger signals were detected in the SGNs of the mNGF-treated group than in the vehicle group at the three time points.
(F) Immunostaining of APAF1 in SGNs of the basal turns of cochleae in DBA/2J mice. APAF1 was more expressed in the vehicle group than in the mNGF-treated group at the three time points. n=3, Scale bar=50 μm.

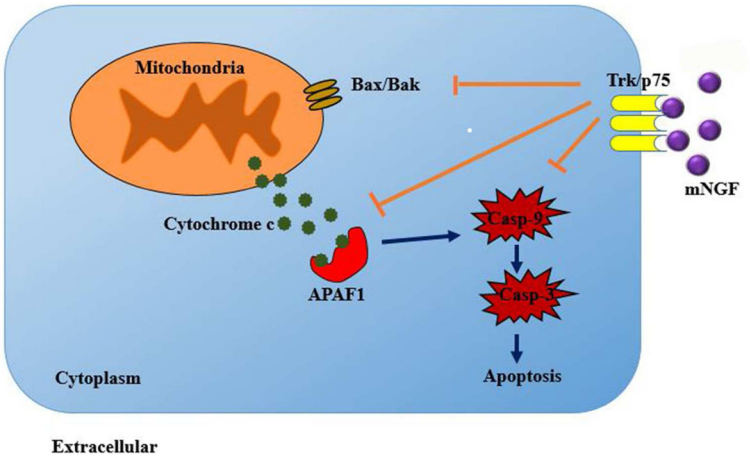

Figure 7.

Conceptual model of mNGF inhibiting apoptosis through the Bak-dependent mitochondrial pathway. Exogenous mNGF can bind with Trk and p75 on the surface membranes of cells, then become phosphorylated and send a signal downstream, inhibiting the expression of pro-apoptotic proteins BAK, BAX and, as a result, reducing the release of mitochondrial cytochrome C, decreasing the expression of caspase-9 and caspase-3, and ultimately inhibiting apoptosis. Bak: Bcl-2-antagonist killer1, Bax: Bcl-2-associated X protein, APAF1: Apoptosis protease activating factor 1.

Table 1

Real-time PCR primer sequence.

Gene	Stand	Sequence (5′–3′)	Gene bank accession number
GAPDH	Forward	TCGTCCCGTAGACAAAATGG	NM_008084.3
	Reverse	TTGAGGTCAATGAGGGGGTC	
BAK1	Forward	AAAATGGCATCTGGACAAGG	NM_007523.2
	Reverse	AGACCTCCTCTGTGTGTCCTGG	
BAX	Forward	TTGCTGATGGCAACTTCAAC	NM_007527.3
	Reverse	GATCAGCTCGGGCACTTTAG	
Caspase-3	Forward	TGTCATCTCGCTCTGGTACG	NM_009810.3
	Reverse	AAATGACCCCTTCATCACCA	
Caspase-9	Forward	CCTAGTGAGCGAGCTGCAAG	NM_001277932.1
	Reverse	ACCGCTTTGCAAGAGTGAAG	